Instabilities due to a heating spike

M. C. Navarro[1], A. M. Mancho[2] and H. Herrero[1]

[1] Departamento de Matemáticas. Facultad de Ciencias Químicas. Universidad de Castilla-La Mancha, 13071 Ciudad Real, Spain.
[2] Instituto de Matemáticas y Física Fundamental, Consejo Superior de Investigaciones Científicas,Serrano 121, 28006 Madrid, Spain.

Abstract.   We study numerically instabilities developed in a fluid layer with a free surface, in a cylindrical container which around the origin at the bottom has a heating spike modelled by a parameter β. Axysimmetric basic states appear as soon a non-zero horizontal temperature gradient is imposed. These states are characterized by the presence of a hot boundary layer in the center and a convective motion in the whole cell. The basic states may bifurcate to different solutions depending on the parameters of the problem. We consider the small aspect ratio and high localization case. Waves (spirals) or stationary patterns with low wave numbers appear after the bifurcation. They are more localized depending on the localization of the heating.

1. Introduction

Instabilities and pattern formation in buoyant flows have been extensively studied in recent years. Classically, heat is applied uniformly from below [1] and the conductive solution (also called the basic solution) becomes unstable for a critical vertical temperature gradient beyond a certain threshold. A more general setup for Rayleigh-Bénard convection than the case of uniform heating, consists of a basic dynamic flow imposed by a non-zero horizontal temperature gradient which may be either constant or not. Numerical results obtained at the former setup in an annular domain address the importance of both vertical and horizontal temperature gradients in the development of instabilities [2, 3, 4, 5]. In this work we consider a cylidrical domain with a localised Gaussian-like heating at the bottom. Therefore, apart from vertical and horizontal temperature gradients, a heat parameter related to the shape of the heating profile at the bottom is introduced. This problem is studied in Ref. [6] in a less localised case where it is shown many different types of instabilities may appear depending on the basic flow and external parameters: giant single armed spiral waves, targets, stationary and oscillatory patterns with different wave numbers extended or localized. In this paper we consider a smaller aspect ratio and higher localization (as a spike). In this case very localised spirals and targets with low wave numbers appear after the bifurcation. They are more localized depending on the localization of the heating. This problem is relevant for geophysics applications as thermal plumes [7].

The paper is organized as follows. Section 2 describes the physical setup, the general mathematical formulation of the problem in a dimensionless form, for basic solutions and their linear stability analysis. Section 3 explains the numerical results on both, the basic and growing perturbations. Finally in section 4 the conclusions are presented.

2. Formulation of the problem

The physical set up (see figure 1) consists of a horizontal fluid layer in a cylindrical container of radius l (r coordinate) and depth d (z coordinate). The upper surface is open to the atmosphere and the bottom plate is rigid. At $z = 0$ the imposed temperature is a Gaussian profile which takes the value $T_{\max}$ at $r = 0$ and the value $T_{\min}$ at the outer part ($r = l$). The environmental temperature is T_0. We define $\triangle T_v = T_{\max} - T_0$, $\triangle T_h = T_{\max} - T_{\min}$ and $\delta = \triangle T_h / \triangle T_v$.

In the equations governing the system u_r, u_ϕ and u_z are the components of the velocity field u, T is the temperature, p is the pressure, r is the radial coordinate and t is the time. The magnitudes are expressed in dimensionless form after rescaling in the following form: $\mathbf{r}' = \mathbf{r}/d$, $t' = \kappa t/d^2$, $u' = du/\kappa$, $p' = d^2 p/ (\rho_0 \kappa \nu)$, $\Theta = (T - T_0)/\triangle T$. Here $\mathbf{r}$ is the position vector, κ

the thermal diffusivity, ν the kinematic viscosity of the liquid and ρ_0 is the mean density at the environment temperature T_0. After reescaling the domain $\Omega_1 = [0, l] \times [0, d]$ is transformed into $\Omega_2 = [0, \Gamma] \times [0, 1]$ where $\Gamma = l/d$ is the aspect ratio

The system evolves according to the momentum and the mass balance equations and to the energy conservation principle, which in dimensionless form are (the primes in the corresponding fields have been dropped),

$$\nabla \cdot u = 0, \tag{1}$$

$$\partial_t \Theta + u \cdot \nabla \Theta = \nabla^2 \Theta, \tag{2}$$

$$\partial_t u + (u \cdot \nabla) u = \mathrm{Pr} \left(-\nabla p + \nabla^2 u + \mathrm{R} \Theta e_z \right), \tag{3}$$

where the operators and fields are expressed in cylindrical coordinates and the Oberbeck-Bousinesq approximation has been used. Here e_z is the unit vector in the z direction. The following dimensionless numbers have been introduced: the Prandtl number $\mathrm{Pr} = \nu/\kappa$ and the Rayleigh number $\mathrm{R} = g\alpha \triangle T d^3/\kappa\nu$, which represents the buoyant effect. In these definitions α is the thermal expansion coefficient and g is the gravity constant.

We discuss now the boundary conditions (bc). The top surface is flat, which implies the following condition on the velocity,

$$u_z = 0, \quad \text{on} \ z = 1. \tag{4}$$

and free slip,

$$\partial_z u_r = 0, \quad \partial_z u_\phi = 0, \quad \text{on} \ z = 1. \tag{5}$$

Lateral and bottom walls are rigid, so

$$u_r = u_\phi = u_z = 0, \quad \text{on} \ z = 0, \tag{6}$$

$$u_r = u_\phi = u_z = 0, \quad \text{on} \ r = \Gamma. \tag{7}$$

For temperature we consider the dimensionless form of Newton's law for heat exchange at the surface,

$$\partial_z \Theta = -B\Theta, \quad \text{on} \ z = 1, \tag{8}$$

where B is the Biot number. At the bottom a gaussian profile is imposed,

$$\Theta = 1 - \delta(e^{(\frac{1}{\beta})^2} - e^{(\frac{1}{\beta} - (\frac{x}{\Gamma})^2 \frac{1}{\beta})^2})/(e^{(\frac{1}{\beta})^2} - 1) \quad \text{on} \ z = 0, \tag{9}$$

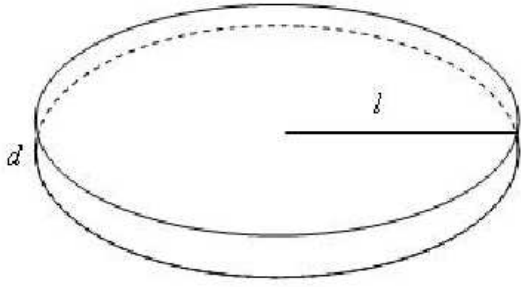where β is a measure of the sharpness of the profile. In figure 2 several plots of this profile for
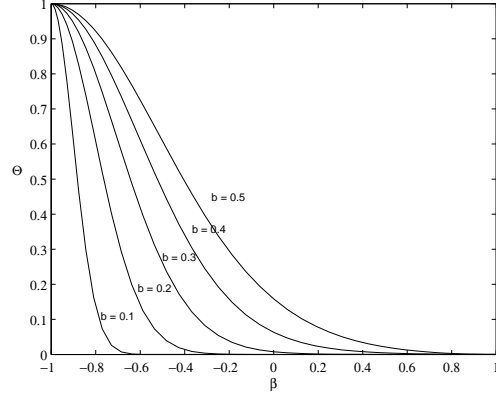
Figure 1. Physical set-up.

Figure 2. Temperature boundary conditions at the bottom for $\Gamma = 5$, $\delta = 1$ and different values of β.

different values of the parameters can be seen. The lateral wall is insulating,

$$\partial_r \Theta = 0 \quad \text{on} \quad r = \Gamma. \tag{10}$$

The use of cylindrical coordinates, which are singular at $r = 0$, requires regularity conditions on velocity, pressure and temperature fields. In general, these conditions are expressed as follows [10]

$$\frac{\partial(u_r e_r + u_\phi e_\phi)}{\partial \phi} = \partial_\phi u_z = \partial_\phi p = \partial_\phi \Theta = 0 \quad \text{on} \quad r = 0, \tag{11}$$

where e_r and e_ϕ are the unit vectors in the r and ϕ directions respectively. To summarize, the dimensionless equations contains these external parameters $(\mathrm{R}, \Gamma, \mathrm{Pr}, \delta, B, \beta)$. Our aim is to describe the type of bifurcations that appear for small values of β (high localization) taking R as bifurcation parameter and fixed values of the rest of the parameters: $\Gamma = 5$, $\mathrm{Pr} = 0.4$, $\delta = 1$ and $B = 0.05$.

2.1. Basic state and linear stability analysis

The horizontal temperature gradient at the bottom (i.e, $\delta \neq 0$) settles a stationary convective motion which is called basic state. It is a time independent solution to the stationary problem obtained from equations (1-3). The basic state is axisymmetric therefore it depends only on $r - z$ coordinates (i.e. all ϕ derivatives are zero). The velocity field of the basic flow is restricted to $u = (u_r, u_\phi = 0, u_z)$. Regularity conditions (11) now become

$$u_r = \partial_r u_z = \partial_r p = \partial_r \Theta = 0 \quad \text{on} \quad r = 0. \tag{12}$$

We have solved numerically the simplified equations for the basic state together with its boundary conditions. We use a Chebyshev collocation method with details given in section Ref. [6].

The stability of the basic state is studied by perturbating it with a vector field depending on the r, ϕ and z coordinates, in a fully 3D analysis, for instance:

$$u_r(r, \phi, z) = u_r^b(r, z) + \bar{u}_r(r, z) \exp(ik\phi + \lambda t), \tag{13}$$

and similarly for u_ϕ, u_z, Θ and p. Here the superscript b indicates the corresponding quantity in the basic state and the bar refers to the perturbation. We have considered Fourier mode expansions in the angular direction, because along it boundary conditions are periodic. Expressions (13) are replaced into basic equations (1-3) and the resulting system is linearized. Boundary conditions for perturbations $(\bar{u}_r, \bar{u}_\phi, \bar{u}_z, \overline{\Theta}, \overline{p})$ are found by substituting (13) into (4-11). Regularity conditions (11) depend now on the wavenumber k:

$$\bar{u}_r = \bar{u}_\phi = \frac{\partial \bar{u}_z}{\partial r} = \frac{\partial \overline{\Theta}}{\partial r} = \frac{\partial \overline{p}}{\partial r} = 0, \text{ for } k = 0, \tag{14}$$

$$\bar{u}_r + i\bar{u}_\phi = \bar{u}_z = \overline{\Theta} = \overline{p} = 0, \text{ for } k = 1, \tag{15}$$

$$\bar{u}_r = \bar{u}_\phi = \bar{u}_z = \overline{\Theta} = \overline{p} = 0, \text{ for } k \neq 0, 1. \tag{16}$$

The resulting problem is an eigenvalue problem in λ. If $Re(\lambda) < 0$ for all eigenvalues the basic state is stable while if there exists a value of λ such as $Re(\lambda) > 0$ the basic state becomes unstable. The condition $Re(\lambda) = 0$ may be satisfied for certain values of the external parameters, $(R, \Gamma, Pr, \delta, B, \beta)$, which define the critical threshold. At the critical threshold, a stationary bifurcation takes place if $Im(\lambda) = 0$ while it is a Hopf bifurcation if $Im(\lambda) \neq 0$.

We have solved both the basic state and the linear stability problem as stated in (1-3), i.e. in primitive variables formulation by expanding the fields with Chebyshev polynomials (see Ref. [8]). Using this technique, the problem of the spurious modes for pressure arises [8, 9], which we have solved using the method proposed in [10], taking additional boundary conditions. They are obtained by the continuity equation at $z = 0$ and the normal component of the momentum equations on $r = \Gamma$ and $z = 1$.

We have solved numerically the stationary axisymmetric version of equations (1-3) together with the boundary conditions, by treating the nonlinearity with a Newton-like iterative method as it is explained in Ref. [6].

The eigenvalue problem is discretized by expanding pertubations (13) in a truncated series of orthonormal Chebyshev polynomials as we did with the basic state. These expressions are replaced into the linearized version of equations (1-3) and boundary and regularity conditions

Table 1. Critical Rayleigh numbers R_c for different orders of expansions in Chebyshev polynomials. The critical wave number is $k_c = 2$ oscillatory and the parameters are $\Gamma = 5$, $Pr = 0.4$, $\delta = 1$, $B = 0.05$ and $\beta = 0.3$.

	$N = 9$	$N = 11$	$N = 13$	$N = 15$
$L = 33$	$5.52 \cdot 10^5$	$6.62 \cdot 10^5$	$7.16 \cdot 10^5$	$7.15 \cdot 10^5$
$L = 35$	$5.85 \cdot 10^5$	$6.79 \cdot 10^5$	$7.34 \cdot 10^5$	$7.30 \cdot 10^5$
$L = 37$	$5.59 \cdot 10^5$	$6.64 \cdot 10^5$	$7.35 \cdot 10^5$	$7.31 \cdot 10^5$
$L = 39$	$5.54 \cdot 10^5$	$6.60 \cdot 10^5$	$7.31 \cdot 10^5$	$7.29 \cdot 10^5$

(4-11). We use a collocation method where equations are evaluated at the Gauss-Lobatto points. Evaluation rules are explained in Ref. [6]. The eigenvalue problem is then transformed into its discrete form

$$Aw = \lambda Bw \tag{17}$$

where w is a vector which contains P unknowns and A and B are $P \times P$ matrices. The discrete eigenvalue problem (17) has a finite number of eigenvalues λ_i. The stability condition previously explained must be required now upon $\lambda_{\max}$ where $\lambda_{\max} = \max Re(\lambda_i)$. In Ref. [11] many details on how to solve this problem efficiently are given.

As in [3], we have carried out a test on the convergence of the method that let us assure the correctness of the results. Table I shows some results on convergence rates. We find that expansions of order 33×9 are enough to ensure accuracy within 1%.

3. Numerical Results

In this section we describe numerical results found for $\Gamma = 5$ and small values of the shape coefficient β ($\beta \in [0.1, 0.5]$). We restringe ourselves to this range due to convergence properties of the numerical method, as β decreases convergence becomes worse. An special treatment of the problem with a specific change of variables to improve convergence properties will be addressed in future work.

We have solved numerically the stationary axisymmetric version of equations (1-3) together with the boundary conditions, as explained in section Ref. [6]. The basic states are formed by hot boundary layers near the center that become more localized when β decreases (see figures 3a and 4a). Those layers generates convective motions in the whole cell with strong velocities near the center (see figures 3b and 4b).

We have studied numerically the linear stability of the numerical basic states following explanations of Ref. [6]. We consider the external parameter R as control parameter. By control parameter we mean the parameter that changed leads to an instability while all the
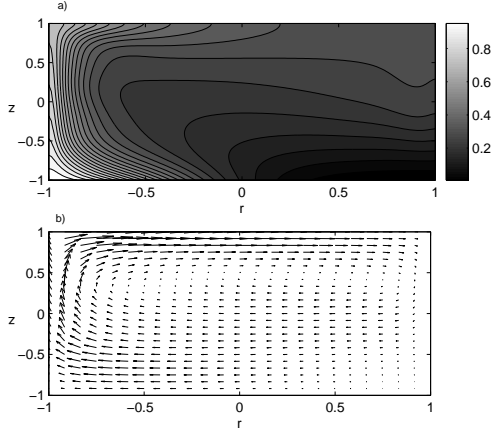
Figure 3. a) Isotherms of the basic state corresponding to values of the parameters $\beta = 0.5$, R $= 1.8 \cdot 10^5$, $\Gamma = 5$, Pr $= 0.4$, $B = 0.05$ and $\delta = 1$; b) velocity field of the basic state for the same values of the parameters.
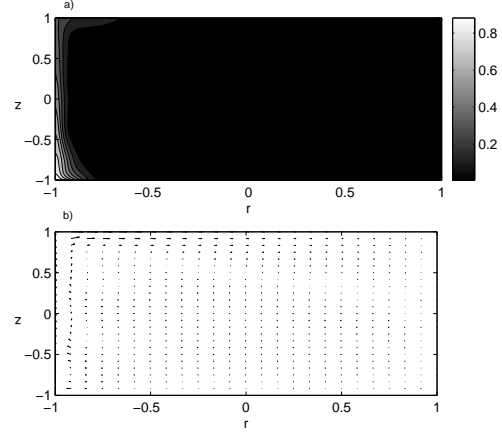

Figure 4. a) Isotherms of the basic state corresponding to values of the parameters $\beta = 0.1$, R $= 5.8 \cdot 10^5$, $\Gamma = 5$, Pr $= 0.4$, $B = 0.05$ and $\delta = 1$; b) velocity field of the basic state for the same values of the parameters.

others are fixed ($\Gamma = 5$, Pr $= 0.4$, $B = 0.05$ and $\delta = 1$). This occurs when $\lambda_{\max}(\text{R})$ changes from a negative value to a positive one as R varies. The value of R_c for which $\lambda_{\max}(\text{R}_c) = 0$ is the critical value. Figure 5 displays $\lambda_{\max}(\text{R}_c)$ as a function of the wave number k and all other parameters fixed. The eigenvalue with maximum real part corresponds to $k = 3$ and as it is complex, the bifurcation is oscillatory. Depending on the parameters different instabilities are obtained either stationary or oscillatory with different growing modes, which are analyzed next.

We study how the shape factor β affect to the instabilities. Figure 6 displays critical values of R_c as a function of β. Critical wave numbers k_c and the corresponding growing modes are shown in this figure where void circles correspond to stationary bifurcations while crossed ones stand for oscillatory instabilities. The critical R_c increases as β decreases till it presents a maximum at $\beta = 0.2$ and it decreases at $\beta = 0.1$ where the bifurcation becomes stationary. As β decreases the critical wave number decreases. The growing modes are spiraled in the Hopf bifurcation cases and it is a target in the stationary bifurcation. The critical eigenfunctions become more localized as β decreases. In the $r - z$ plane for the growing modes two types are observed: for medium β (0.2-0.5) a hot boundary layer is formed in the center of the cylinder where the heating is applied (see figure 7a), that corresponds to an oscillatory bifurcation; and for small β (0.1) a cold boundary layer is formed in the center (see figure 8a) which corresponds to a stationary bifurcation. Those layers generate some convective motions in the $r - z$ plane in the whole layer (see figures 7b and 8b).
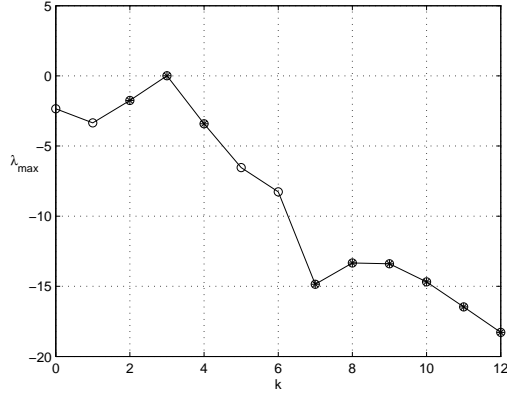
Figure 5. Maximum real part of the growth rate λ as a function of k for basic state at threshold $R_c = 1.8 \cdot 10^5$, the rest of the parameters are $\Gamma = 5$, $Pr = 0.4$, $B = 0.05$, $\delta = 1$ and $\beta = 0.5$. The maximum determines the critical $k_c = 3$. Void circles correspond to real eigenvalues while crossed ones stand for complex eigenvalues.
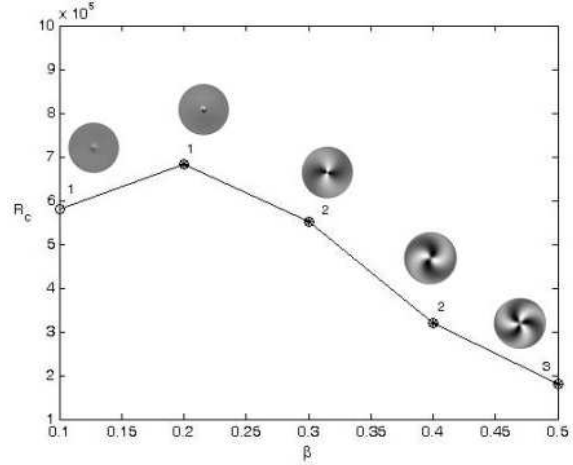

Figure 6. Critical R, wave number k values and growing modes as a function of β for $\delta = 1$. Remaining external parameters are $\Gamma = 5$, $Pr = 0.4$ and $B = 0.05$. Void circles correspond to stationary instabilities while crossed ones stand for oscillatory instabilities.
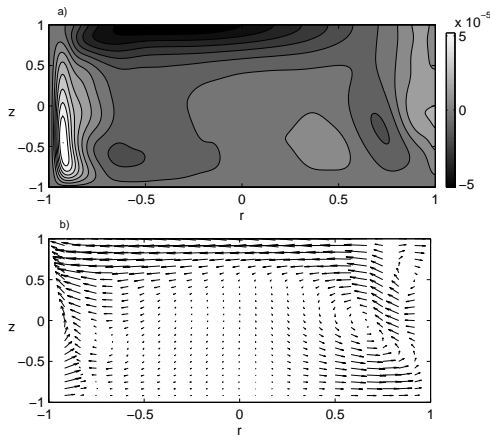

Figure 7. a) Isotherms of growing mode eigenfunction in the $r-z$ plane corresponding to values of the parameters $\beta = 0.5$, R $= 1.8 \cdot 10^5$, $\Gamma = 5$, $Pr = 0.4$, $B = 0.05$ and $\delta = 1$; b) velocity field of the growing mode eigenfunction in the $r-z$ plane for the same values of the parameters.
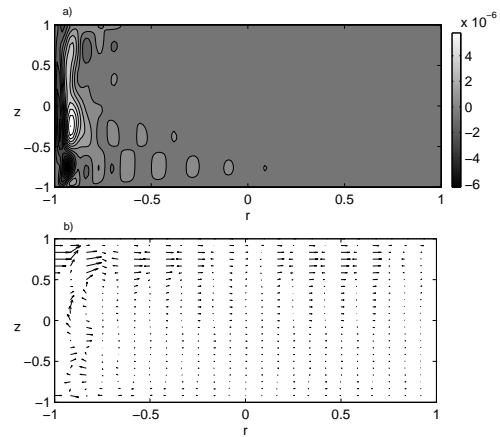

Figure 8. a) Isotherms of growing mode eigenfunction in the $r-z$ plane corresponding to values of the parameters $\beta = 0.1$, R $= 5.8 \cdot 10^5$, $\Gamma = 5$, $Pr = 0.4$, $B = 0.05$ and $\delta = 1$; b) velocity field of the growing mode eigenfunction in the $r-z$ plane for the same values of the parameters.

4. Conclusions

We have studied the stationary and axisymmetric basic states that appear in a Rayleigh-Bénard problem with a heating spike in the bottom which shape is measured by the factor β. They consists of hot boundary layers in the center that generates a convective motion in the whole cell. These states bifurcate to different 3D structures depending on the shape factor β for fixed values of the rest of the parameters. We have found a different behavior between medium values of β and small ones. For medium values of β the bifurcation is oscillatory to spiraled structures. The patterns become more localized and the wave numbers decrease as β decreases. For small values of β the bifurcation is stationary with small wave number $k_c = 1$.

[1] H. Bénard, "Les tourbillons cellulaires dans une nappe liquide. "*Rev. Gén. Sci. Pures Appl.* **11**, 1261 (1900).

[2] A.M. Mancho and H. Herrero, "Instabilities in a lateraly heated liquid layer."*Phys. Fluids* **12**, 1044 (2000).

[3] S. Hoyas, H. Herrero and A.M. Mancho, "Thermal convection in a cylindrical annulus heated laterally. "*J. Phys. A: Math and Gen.* **35**, 4067 (2002).

[4] S. Hoyas, H. Herrero and A.M. Mancho, "Bifurcation diversity of dynamic thermocapillary liquid layers."*Phys. Rev. E*, **66**, 057301 (2002).

[5] S. Hoyas, A.M. Mancho, H. Herrero, N. Garnier, A. Chiffaudel. "Bénard-Marangoni convection in a differentially heated cylindrical cavity"*Phys. Fluids*, **17**, 054104 (2005).

[6] M. C. Navarro, A. M. Mancho and H. Herrero, "Spiral Instabilities in Rayleigh-Bénard Convection under Localized Heating". Submitted to Chaos (2006).

[7] S. Labrosse, "Hotspots, mantle plume and core heat loss". *Earth and Planetary Science Letters*, **199**, 147-156 (2002).

[8] C. Bernardi and Y. Maday. Approximations spectrales de problèmes aux limites elliptiques. Springer-Verlag, Berlin, (1991).

[9] C.Canuto, MY Hussaine, A. Quarteroni, TA Zang. Spectral Methods in Fluid Dynamics. Springer: Berlin, 1988.

[10] H. Herrero and A.M. Mancho, "On pressure boundary conditions for thermoconvective problems."*Int. J. Numer. Meth. Fluids* **39**, 391 (2002).

[11] M.C. Navarro, A. Wathen, A. M. Mancho, H. Herrero. *Journal of Computational Physics* submitted.